Electronic Supplementary Information (ESI)

Ultrathin nanosheets of palladium in boosting its cocatalyst role and plasmonic effect towards enhanced photocatalytic hydrogen evolution

Yuzhen Zhu,[a] Zaixiang Xu,[a] Wenya Jiang,[b] Wenjie Yin,[a] Shuxian Zhong,[a] Peijun Gong,[a] Ru Qiao,[a] Zhengquan Li*[a] and Song Bai*[a,b]

[a] Key Laboratory of the Ministry of Education for Advanced Catalysis Materials, College of Chemistry and Life sciences, Institute of Physical and Chemistry, Zhejiang Normal University, Jinhua, Zhejiang, 321004, P. R. China.
[b] Hefei National Laboratory for Physical Sciences at the Microscale, iChEM (Collaborative Innovation Center of Chemistry for Energy Materials), Hefei Science Center (CAS), and School of Chemistry and Materials Science, University of Science and Technology of China, Hefei, Anhui, 230026, P. R. China.

E-mail: songbai@zjnu.edu.cn; zqli@zjnu.edu.cn

1. Synthetic procedures.

Chemical. K_2PdCl_4 (Aladdin, P106044), Palladium(II) acetylacetonate ($Pd(acac)_2$, Aladdin, P101065), tungsten hexacarbonyl ($W(CO)_6$, Alfa Aesar, 43205) and poly(vinyl pyrrolidone) (PVP, M.W. ≈ 29000, Aldrich, 234257) were used in the synthesis. All other chemicals were of analytical grade and purchased from *Sinopharm Chemical Reagent* Co., Ltd. The water used in all experiments was de-ionized (DI). All chemicals were used as received without further purification.

Synthesis of TiO_2 nanosheets. The TiO_2 nanosheets were synthesized by modifying a method in literature with hydrofluoric acid as a capping agent.[S1] Caution! Hydrofluoric acid is extremely corrosive and toxic, and should be handled with extreme care.

2. Sample characterizations.

Prior to electron microscopy characterizations, a drop of the aqueous suspension of particles was placed on a piece of carbon-coated copper grid and dried under ambient conditions. TEM and HRTEM images were taken on a JEOL JEM-2100F field-emission high-resolution transmission electron microscope operated at 200 kV.

Powder X-ray powder diffraction (XRD) patterns were recorded by using a Philips X'Pert Pro Super X-ray diffractometer with Cu-Kα radiation (λ = 1.5418 Å).

X-ray photoelectron spectra (XPS) were collected on an ESCALab 250 X-ray photoelectron spectrometer, using nonmonochromatized Al-Kα X-ray as the excitation source.

UV-vis-NIR diffuse reflectance data were recorded in the spectral region of 240-1600 nm with a Shimadzu SolidSpec-3700 spectrophotometer. UV-vis-NIR absorption spectra were taken using an Agilent Varien Cary 60 spectrophotometer.

Photoluminescence (PL) spectra were recorded on a Jobin Yvon Horiba Fluorolog-3-Tau Spectrofluorometer.

The molar ratios of Pd to TiO_2 were measured as follows: the TiO_2-Pd samples were dissolved with a mixture of HCl and HNO_3 (3:1, volume ratio), which was then diluted with 1% HNO_3. The concentrations of Pd were then measured with a Thermo Scientific PlasmaQuad 3 inductively-coupled plasma mass spectrometry (ICP-MS). The molar ratios of TiO_2 to Pd were determined by sample weighing prior to the dissolution of Pd for the ICP-MS measurements.

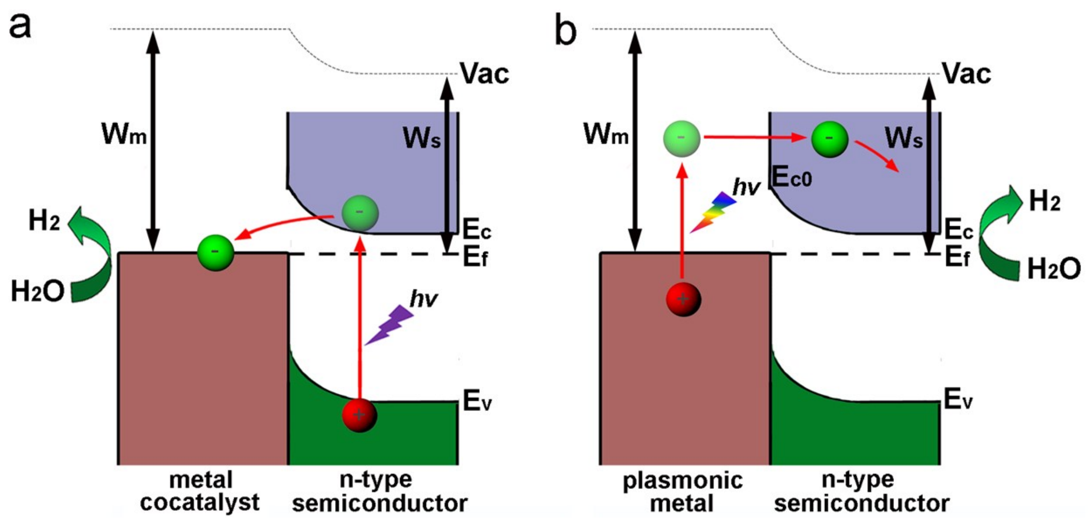

Fig. S1 Schematic band diagrams illustrating the photocatalytic H_2 evolution in the hybrid structures of (a) n-type semiconductor and metal cocatalyst as well as (b) plasmonic metal and n-type semiconductor.

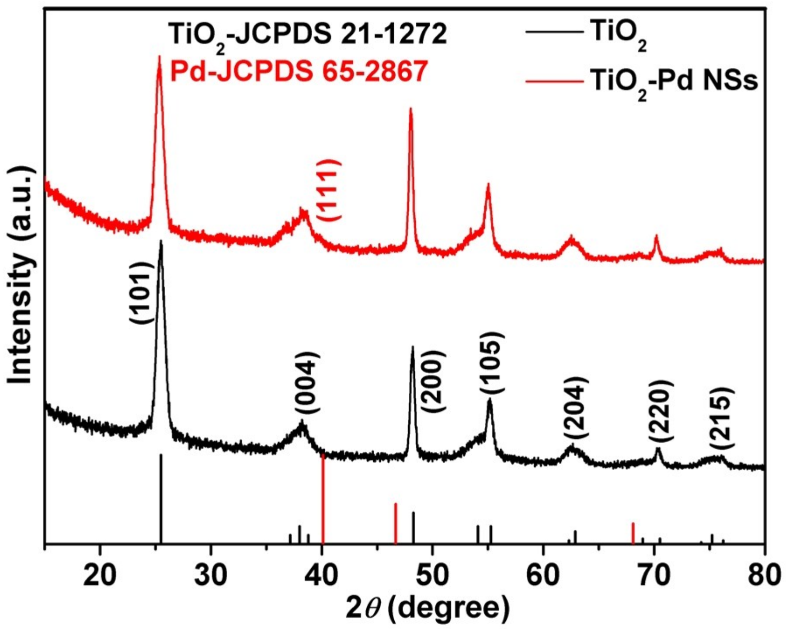

Fig. S2 XRD patterns of TiO_2-Pd NSs in reference to bare TiO_2 nanosheets. The standard diffraction patterns for anatase TiO_2 (JCPDS 21-1272) and *fcc* Pd (JCPDS 65-2867) are provided as references.

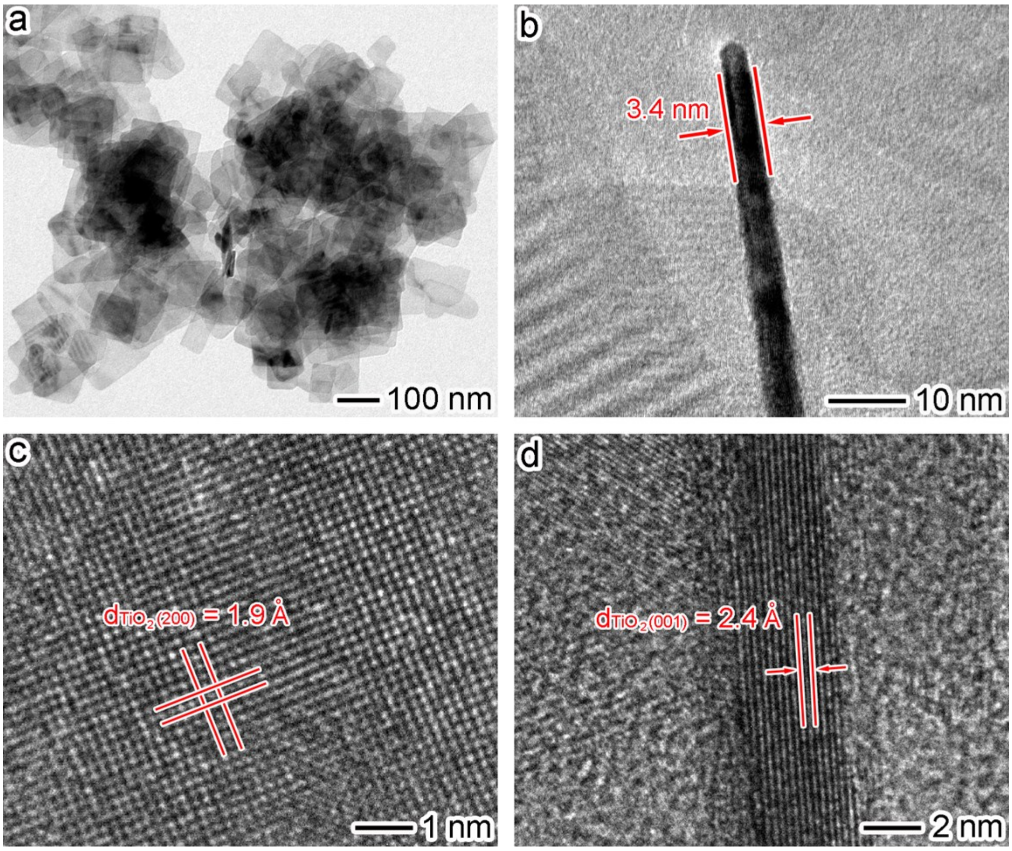

Fig. S3 TEM and HRTEM images of TiO_2 nanosheets: (a) TEM image showing the flat surface of nanosheets; (b) TEM image showing the cross section and thickness of the nanosheets; (c) HRTEM image showing the lattice fringes of the flat faces; (d) HRTEM image showing the lattice fringes of side faces.

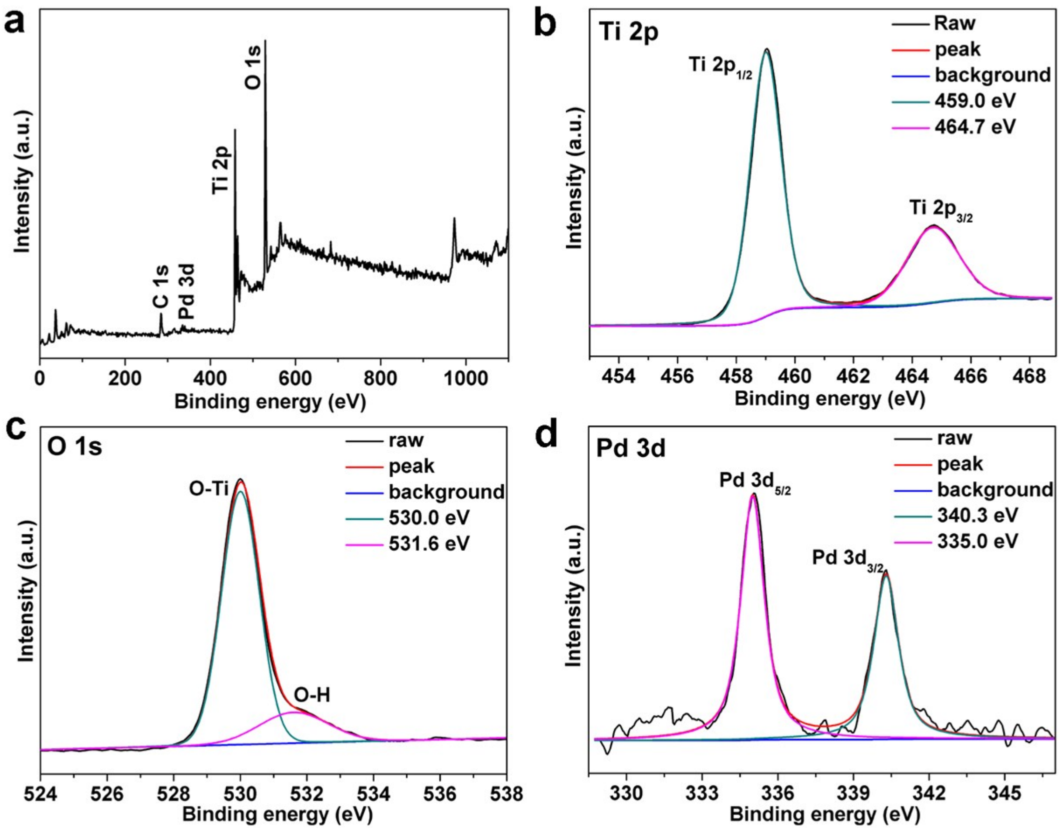

Fig. S4 XPS spectra of TiO_2-Pd NSs: (a) survey spectrum, (b) Ti2p, (c) O1s and (d) Pd3d high-resolution spectra.

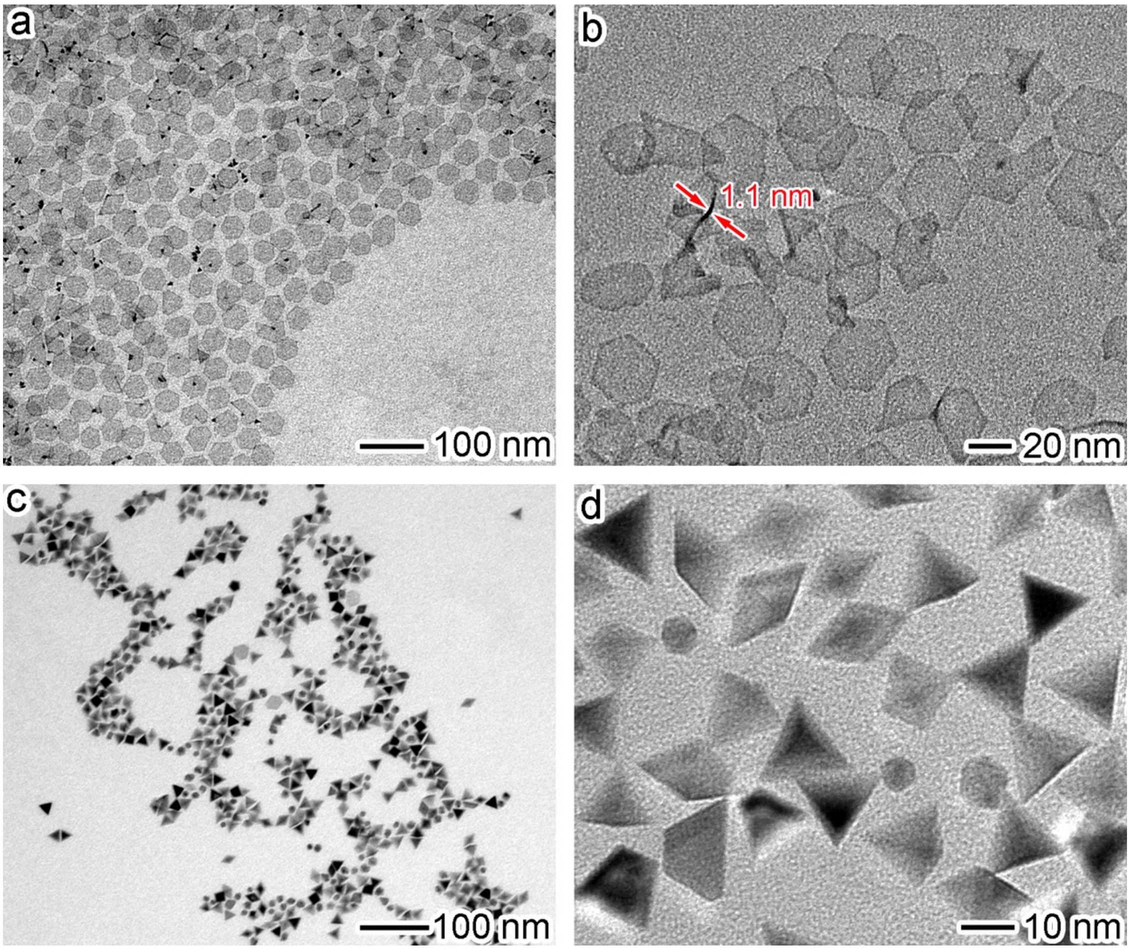

Fig. S5 TEM images of (a,b) bare Pd nanosheets and (c,d) bare Pd nanotetrahedrons.

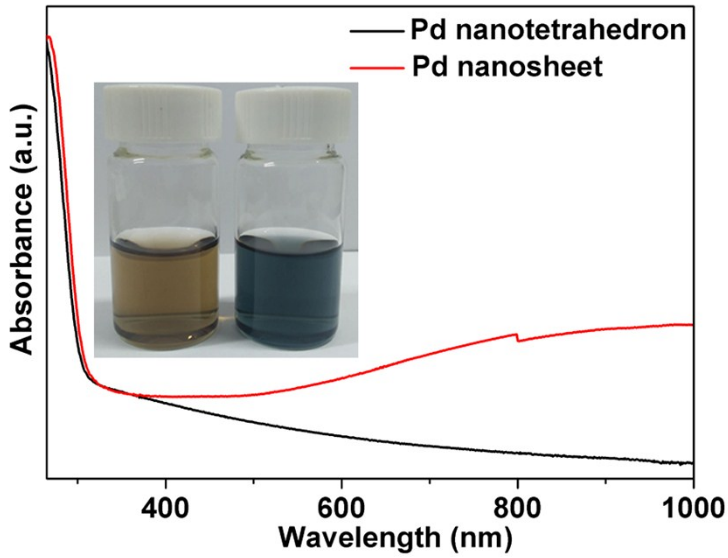

Fig. S6 UV-vis-NIR absorption spectra of Pd nanotetrahedrons and Pd nanosheets, the inset of Fig. S6 is the photograph of aqueous suspensions of Pd nanotetrahedrons and Pd nanosheets.

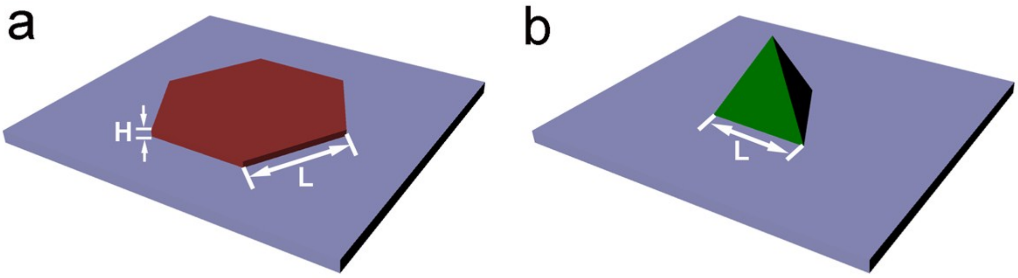

$$V_{Pd} = 6 \times H \times \frac{\sqrt{3}}{4} L^2$$

$$S_{interface} = 6 \times \frac{\sqrt{3}}{4} L^2$$

$$S_{surface} = 6 \times \frac{\sqrt{3}}{4} L^2 + 6 \times L \times H$$

$$V_{Pd} = \frac{\sqrt{2}}{12} L^3$$

$$S_{interface} = \frac{\sqrt{3}}{4} L^2$$

$$S_{surface} = \frac{\sqrt{3}}{4} L^2 \times 3$$

Fig. S7 Schematic illustration showing the calculation of TiO_2-Pd interfacial area and exposed Pd surface area as well as the corresponding interface-to-volume and surface-to-volume ratio of Pd in (a) TiO_2-Pd NSs and (b) TiO_2-Pd NTs, respectively.

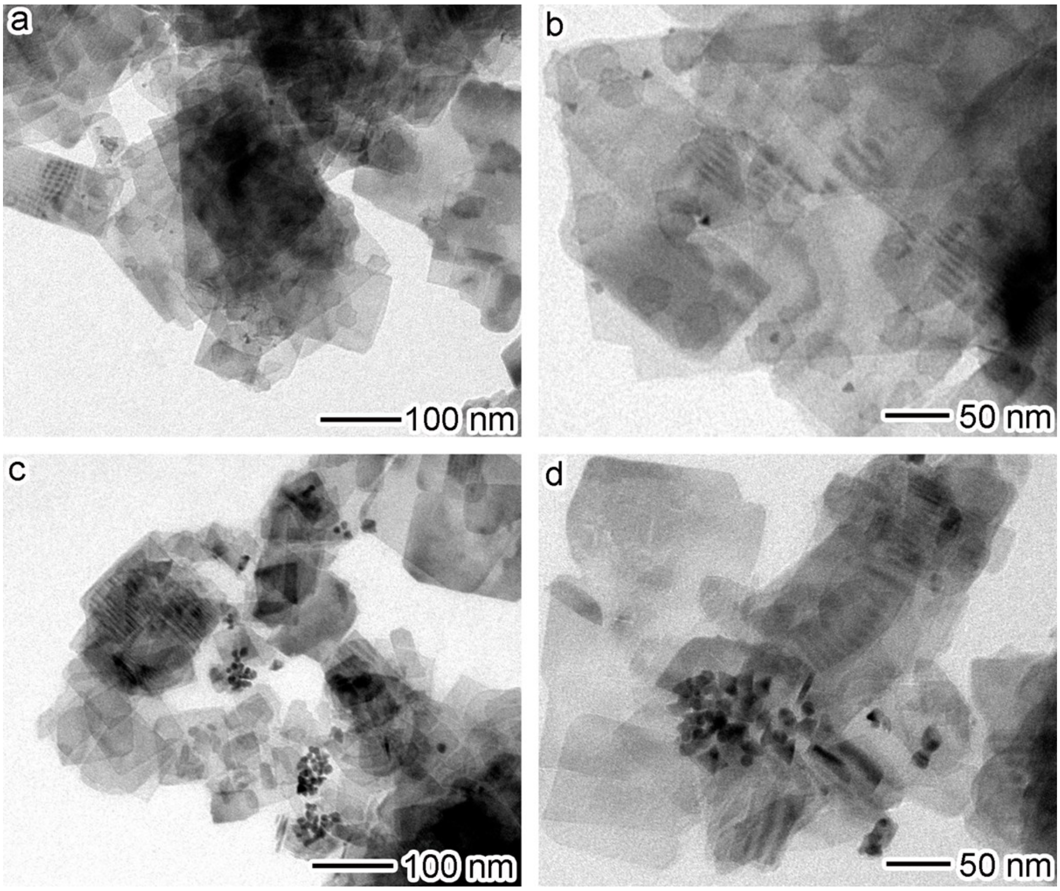

Fig. S8 TEM image of the (a,b) TiO_2-Pd NSs and (c,d) TiO_2-Pd NTs after photocatalytic reaction.

Table S1 Chemical compositions of the TiO_2-Pd samples determined by ICP-MS.

Sample	Weight ratio of Pd : TiO_2
TiO_2-Pd NSs	4.9 : 100
TiO_2-Pd NTs	4.6 : 100

References

S1 X. Han, Q. Kuang, M. Jin, Z. Xie and L. Zheng, *J. Am. Chem. Soc.*, 2009, **131**, 3152.